Isolation and Proteomic Characterization of the Arabidopsis Golgi Defines Functional and Novel Components Involved in Plant Cell Wall Biosynthesis[1][W][OA]

Harriet T. Parsons, Katy Christiansen, Bernhard Knierim, Andrew Carroll, Jun Ito, Tanveer S. Batth, Andreia M. Smith-Moritz, Stephanie Morrison, Peter McInerney, Masood Z. Hadi, Manfred Auer, Aindrila Mukhopadhyay, Christopher J. Petzold, Henrik V. Scheller, Dominique Loqué, and Joshua L. Heazlewood*

Joint BioEnergy Institute and Physical Biosciences Division, Lawrence Berkeley National Laboratory, Berkeley, California 94720 (H.T.P., K.C., B.K., A.C., J.I., T.S.B., A.M.S.-M., S.M., P.M., M.Z.H., M.A., A.M., C.J.P., H.V.S., D.L., J.L.H.); Sandia National Laboratory, Livermore, California 94551 (S.M., P.M., M.Z.H.); and Department of Plant and Microbial Biology, University of California, Berkeley, California 94720 (H.V.S.)

The plant Golgi plays a pivotal role in the biosynthesis of cell wall matrix polysaccharides, protein glycosylation, and vesicle trafficking. Golgi-localized proteins have become prospective targets for reengineering cell wall biosynthetic pathways for the efficient production of biofuels from plant cell walls. However, proteomic characterization of the Golgi has so far been limited, owing to the technical challenges inherent in Golgi purification. In this study, a combination of density centrifugation and surface charge separation techniques have allowed the reproducible isolation of Golgi membranes from Arabidopsis (*Arabidopsis thaliana*) at sufficiently high purity levels for in-depth proteomic analysis. Quantitative proteomic analysis, immunoblotting, enzyme activity assays, and electron microscopy all confirm high purity levels. A composition analysis indicated that approximately 19% of proteins were likely derived from contaminating compartments and ribosomes. The localization of 13 newly assigned proteins to the Golgi using transient fluorescent markers further validated the proteome. A collection of 371 proteins consistently identified in all replicates has been proposed to represent the Golgi proteome, marking an appreciable advancement in numbers of Golgi-localized proteins. A significant proportion of proteins likely involved in matrix polysaccharide biosynthesis were identified. The potential within this proteome for advances in understanding Golgi processes has been demonstrated by the identification and functional characterization of the first plant Golgi-resident nucleoside diphosphatase, using a yeast complementation assay. Overall, these data show key proteins involved in primary cell wall synthesis and include a mixture of well-characterized and unknown proteins whose biological roles and importance as targets for future research can now be realized.

The plant Golgi apparatus is responsible for the biosynthesis of matrix polysaccharides and is involved in the further glycosylation of peptide chains imported from the endoplasmic reticulum (ER; Saint-Jore-Dupas et al., 2006). The Golgi also plays a defining role in the secretory pathway, determining the destination of proteins, lipids, and complex carbohydrates to the cell wall and other organelles (Matheson et al., 2006; Nanjo et al., 2006). Recent years have seen a surge of interest in this area as the importance of the cell wall as a substrate for cellulosic biofuels has been recognized (Blanch et al., 2008). Efficient breakdown of the plant cell wall is an important objective in the manipulation of cell wall biosynthetic pathways. Detailed information on the complex array of processes carried out in the Golgi is crucial to understanding plant growth regulation and, therefore, to the successful manipulation of cell wall synthesis. However, our knowledge of even well-studied pathways such as the biosynthesis of the hemicellulose xyloglucan (Scheible and Pauly, 2004) or even the *N*-glycosylation of proteins (Strasser, 2009) is far from complete. It has been speculated that the biosynthesis of hemicellulose and pectin by various glycosyltransferases (GTs) occurs in specific complexes (Liepman et al., 2005; Scheller et al., 2007; Mohnen, 2008), but partner proteins have yet to be identified. Likewise, little is known concerning the structural modifications of glycosylated proteins, despite the diverse array of glycan structures that are synthesized in plants (Seifert and Roberts, 2007). The plant Golgi is highly dynamic, moving around the plant cell via actin networks (Hawes and Brandizzi, 2004), a process that is likely to be crucial in coordinating the delivery of substrates with cell growth. While a few cytoskeleton-interacting proteins have been identified in Arabidopsis (*Arabidopsis thaliana*; Avisar et al., 2008), such critical features of the plant Golgi are little understood for the most part.

[1] This work was supported by the Office of Science, Office of Biological and Environmental Research, U.S. Department of Energy (contract no. DE–AC02–05CH11231) and by the Alexander von Humboldt Foundation (Feodor Lynen Research Fellowship to B.K.).

* Corresponding author; e-mail jlheazlewood@lbl.gov.

The author responsible for distribution of materials integral to the findings presented in this article in accordance with the policy described in the Instructions for Authors (www.plantphysiol.org) is: Joshua L. Heazlewood (jlheazlewood@lbl.gov).

[W] The online version of this article contains Web-only data.

[OA] Open Access articles can be viewed online without a subscription.

www.plantphysiol.org/cgi/doi/10.1104/pp.111.193151

A range of organelles from the model plant Arabidopsis have been isolated and extensively characterized by mass spectrometry (MS; Baginsky and Gruissem, 2006; Heazlewood et al., 2007), but only a few limited analyses of the plant Golgi apparatus have thus far been undertaken (Asakura et al., 2006; Dunkley et al., 2006). Plant Golgi stacks are notoriously labile, losing their macroarchitecture during homogenization techniques when most other organelles remain intact (Morre and Mollenhauer, 1964). Loss of stack integrity means that the assessment of purity by electron microscopy becomes difficult and differences in density between Golgi membranes and contaminating organelles are less easily exploited (Morre and Mollenhauer, 2009). However, although overall architecture is lost, individual cisternae at least remain intact during gentle homogenization and centrifugation (Munoz et al., 1996).

In plants, the Golgi maintains a close physical relationship with the ER (Boevink et al., 1998). ER membranes are a frequent source of contamination in Golgi vesicle preparations by density centrifugation, as these two membranous structures have similar properties. A comprehensive survey of Golgi enrichment in step gradients, using morphometric analysis of electron micrographs and enzymatic assays, concluded that, in the absence of chemical fixatives such as glutaraldehyde, this technique can yield fractions constituting approximately 50% Golgi material (Morre and Mollenhauer, 2009). Likewise, a combination of downward and flotation centrifugation achieved appreciable enrichment of intact Golgi membranes, but substantial contamination from ER membranes could not be avoided (Gibeaut and Carpita, 1990). Proteomic characterization requires higher levels of purity so that unknown proteins may be assigned with confidence to a given subcellular location. Purity levels are frequently assessed by immunoblotting and enzyme assays. As information is gathered from a limited set of marker proteins, an accurate estimation of contamination may be difficult using these methods. Although Golgi-enrichment techniques preceded proteomics by some decades, the purity of preparations has so far been the principal restriction for proteomic characterization of the plant Golgi.

Few proteomic characterizations of isolated plant Golgi membranes have thus far been undertaken (Asakura et al., 2006). Previous work, however, has demonstrated the potential for informative proteomic analyses of Golgi membranes without recourse to direct organelle isolation (Dunkley et al., 2004, 2006). These latter studies showed partial separation of Golgi and ER along a linear density gradient using immunoblotting with organelle-specific markers. Isotope-tagged proteins were grouped according to their relative distribution patterns along this gradient, from which 89 proteins were assigned to the Golgi and 182 to the ER (Dunkley et al., 2006). This study marked the first sizable contribution to the Golgi and ER proteomes and outlines a core set of Golgi proteins. Analyses by localization of organelle proteins by isotope tagging focused on membrane-bound proteins; a subtly different protein subset identified by the analysis of intact cisternae could identify further novel Golgi proteins, while membrane proteins identified using both methods would provide mutual validation of techniques. Therefore, although proteomic studies and fluorescent protein localization have in combination localized over 170 proteins to the Golgi, a robust technique that permitted the isolation of Golgi cisternae at sufficiently high purity levels for proteomic and/or biochemical analyses would be of great benefit.

In addition to density centrifugation, organelles can also be separated by surface charge (Canut et al., 1999). The specific protein and lipid constituents of membranes result in variation in surface charge between organelles and therefore different migration distances in an electric field. These characteristics are exploited by free-flow electrophoresis (FFE), in which a mixture of membranes and organelles is introduced into a chamber, moving up under laminar flow while an electric field is applied at right angles to the direction of flow (Islinger et al., 2010). In combination with other organelle-enrichment techniques, FFE has been used successfully in the preparation of a variety of organelles from several plant species, including tonoplast and plasma membrane vesicles at high levels of purity, but to date has not been used in the isolation of Golgi vesicles (Canut et al., 1988, 1990; Bardy et al., 1998). Importantly, it has now also been demonstrated that the FFE technique can be very successfully applied to the separation of organelles with similar surface charges such as mitochondria and peroxisomes, which could not be easily separated in the past by other techniques (Eubel et al., 2008; Huang et al., 2009).

In this study, to our knowledge for the first time, intact Golgi membranes from Arabidopsis have been purified to a sufficient level of purity for proteomic characterization through a combination of density centrifugation and surface charge separation techniques (FFE). The in-depth characterization of the plant Golgi by MS has robustly identified 491 proteins from three independent preparations. These results will help identify novel components of cell wall synthesis and regulatory networks, which will greatly assist the development of cell wall manipulation strategies for biofuel production.

RESULTS

Enrichment of Golgi Membranes from Arabidopsis Cell Culture

Enzymatic digestion of cell walls permits the delicate homogenization of Arabidopsis cells, which increases the structural preservation of organelles released during cell rupture (Eubel et al., 2008). This is

paramount in the case of the Golgi, whose heterogeneous structure had contributed to experimental difficulties historically encountered during attempts at its isolation. Low-speed centrifugation removed denser contaminants such as plastid, nuclei, and the majority of mitochondria (data not shown). Golgi membranes in the resulting supernatant were further enriched using established density centrifugation techniques (Morre and Mollenhauer, 2009). Relative enrichment for Golgi membranes versus contaminants during this process was tracked using the cis-Golgi marker α-mannosidase I (α-ManI). With the exception of the ER (calreticulin [CRT1]), major contaminants were depleted during centrifugation prior to analysis by FFE, as observed in the pre-FFE fraction by immunoblotting (Fig. 1). However, despite the reduction in contamination shown by immunoblotting, liquid chromatography (LC)-tandem mass spectrometry (MS/MS) analysis and quantification by spectral counting of the 0.75/1.0 M interface (pre-FFE) showed a continued presence of contaminants; of those for which a subcellular location could be confidently ascertained from organelle marker proteins, 34% were identified as contaminants and only 24% as Golgi localized (Supplemental Fig. S1A), indicating that further purification was required for reliable proteomic analysis of Golgi membranes.

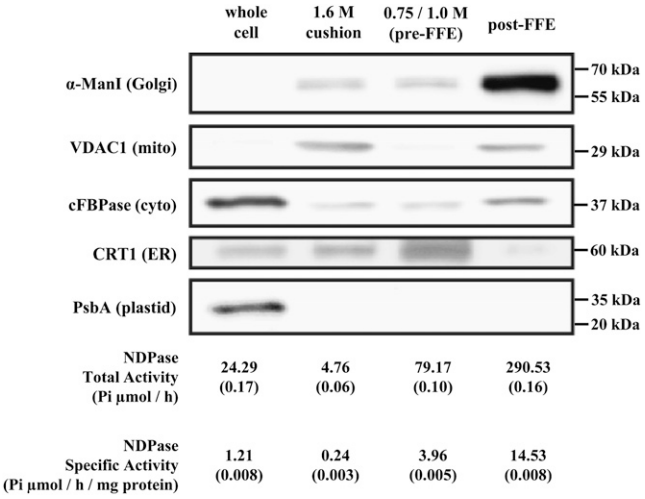

Figure 1. Assessment of the progressive enrichment of Golgi membranes. Samples (10 μg) from each stage of the purification process were analyzed by immunoblotting with membrane markers to principal contaminating organelles. Antibodies represent the following: α-ManI, cis-Golgi marker; VDAC1, mitochondrion; cFBPase (cytosolic Fru-1,6-bisphosphatase), cytosol; CRT1, ER; PsbA (PSII protein D1), plastid. Whole cell is total cellular protein; 1.6 M cushion is the enriched sample prior to the Suc density gradient; 0.75/1.0 M is the enriched Golgi fraction after the Suc gradient (pre-FFE); post-FFE is up to five pooled fractions after separation by FFE. For NDPase activity, a total of 20 μg of protein from each step in the purification procedure was measured for inorganic phosphate (Pi) release using the malachite green colorimetric assay. Values are from three independent experiments (n = 3) expressed as total activity and specific activity with SE values shown in parentheses.

Purification of Golgi Membranes by FFE

The enriched Golgi fraction from the 0.75/1.0 M Suc interface was loaded at the anode injection port of the FFE device. Fractions were collected on 96-well plates, combined, and concentrated by ultracentrifugation. Highly purified post-FFE Golgi fractions were determined by analyzing approximately 10 fractions (between 15 and 25) by LC-MS/MS and profiling the identified proteins using organelle marker proteins (Heazlewood et al., 2007). Due to numerous technical considerations, slight variations in migration occur between experiments, although A_{280} profiles enable accurate estimations for profiling by LC-MS/MS. The post-FFE Golgi-purified fractions comprised two to three sequential fractions (always between fractions 15 and 25), which contained abundant Golgi markers and minimal contaminating proteins. The efficacy of FFE as an orthogonal enrichment strategy is evident from the decrease in CRT1 and the striking increase in α-ManI in the highly enriched post-FFE fraction (Fig. 1). No significant changes were observed in the proportion of contaminants, protein synthesis proteins, or transitory proteins (vacuolar, plasma membrane, and extracellular proteins) based on their relative abundances. Significantly, among proteins of definable subcellular locations, the proportion of experimentally determined Golgi proteins dramatically increased (from 24% to 51%) after FFE, while contaminants and transients decreased from 34% and 28% to 20% and 19%, respectively. Protein synthesis proteins showed a smaller decline, from 14% to 10% (Supplemental Fig. S1). The electrophoretic migration of Golgi and principal contaminants (ER and mitochondria) was also monitored by immunoblotting (Fig. 2). As predicted from the electrophoretic migration of mammalian Golgi, plant Golgi membranes were marginally more electronegative than many of the other contaminating membranes (Morre and Mollenhauer, 1964). Accordingly, the cis-Golgi marker α-ManI was detected in more anodic fractions (16–29), peaking at fraction 18 (Fig. 2). Signal intensity for the ER marker CRT1 and the mitochondrial marker porin (Voltage-Dependent Anion Channel1 [VDAC1]) was greater across fractions 20 to 48 and 22 to 29, respectively (Fig. 2). Latent nucleoside diphosphatase (NDPase) activity, a frequently used Golgi marker, was used to further assess purity after FFE. Around five fractions (equivalent to fractions 15–19 in Fig. 2) were pooled and assayed. An approximately 12-fold increase was observed between whole cell lysates and the pooled post-FFE fractions, while an approximately 60-fold increase was identified between post low-speed centrifugation (1.6 M cushion) and the pooled post-FFE fractions (Fig. 1). Taken together, these data demonstrate substantial Golgi enrichment from whole cell fractions by a combination of successive density centrifugation and FFE.

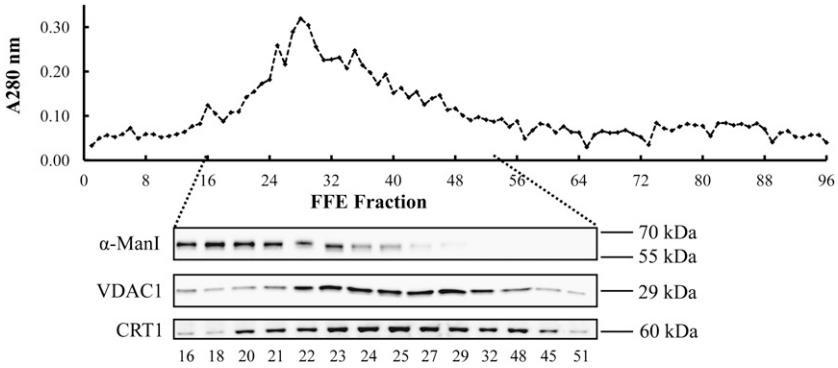

Figure 2. Organelle migration during FFE as determined by immunoblotting. The distribution of total protein was determined using A_{280} measurements. Representative fractions were separated by SDS-PAGE and analyzed by immunoblotting with subcellular markers. The distribution of organelle markers for Golgi (α-ManI), mitochondria (VDAC1), and the ER (CRT1) after FFE separation demonstrated that the Golgi could be further separated from the enriched fraction. A post-FFE purified Golgi sample would typically consist of the region highlighted by fractions 16 to 18 or the equivalent, depending on A_{280} output. These samples would be either pooled for immunoblotting/enzyme analysis or analyzed independently by LC-MS/MS for proteomic characterization.

Electron Microscopy of Purified Golgi Membranes

Maintenance of the structural integrity of Golgi-derived vesicles was important, as vesicle orientation affects migration during electrophoresis. The structure of the Golgi apparatus was tracked throughout the purification procedure using electron microscopy. Protoplasts derived from 7-d-old cells appeared healthy and contained numerous Golgi stacks (Fig. 3A). Golgi stacks are fragile, typically only remaining intact during density centrifugation if low concentrations of glutaraldehyde are added to homogenization buffers (Morre and Mollenhauer, 2009). Cisternae in loosely aggregated stacks were observed in the homogenate in close proximity to densely staining structures of similar dimensions to individual cisternae (Fig. 3B), suggesting that some unstacking was occurring despite the gentle homogenization technique. The presence of partially unstacked cisternae implies that loss of cisternal structure was not widespread, despite the loss of stack macroarchitecture. The Golgi-enriched fraction centrifuged onto the 1.6 M Suc cushion was rich in mitochondria (data not shown) and also contained densely staining, membranous structures of 300 to 600 μm in length (Fig. 3C). Due to technical constraints, immunogold labeling of these structures was not possible and hence unequivocal identification of these structures as cisternae was not undertaken, but similarities in dimensions and appearance to the loosely stacked cisternae (Fig. 3B) and previously isolated plant Golgi cisternae (Morre and Mollenhauer, 1964) strongly supported the cisternal nature of these structures. The 0.75/1.0 M Suc interface also contained many densely staining, membranous structures (Fig. 3D). Immunoblotting and enzyme assays indicated that this fraction was Golgi enriched (Fig. 1), so it is likely that these structures were Golgi derived. Some of these membranous structures resembled those observed on the Suc cushion (Fig. 3C), while others were present in loops of 200 to 500 μm diameter (Fig. 3D). Small, bulbous swellings at the ends of the unlooped structures or along the perimeter of looped structures were suggestive of two membranous structures fused together at their ends (Fig. 3D). Fractions from post-FFE analyses contained a dilute but homogenous collection of similar structures of approximately 200 to 400 μm in diameter (Fig. 3E). As these fractions represented the most Golgi-enriched fractions after FFE, it is likely that these are dissociated Golgi stacks. The morphology of individual vesicles was not sufficiently clear to show whether these structures were formed from looped, swollen, or ruptured and reformed cisternae (Fig. 3E).

Analysis of FFE-Purified Golgi Membranes by LC-MS/MS

The analyses outlined above indicated that the FFE could deliver sufficiently highly purified Golgi samples for proteomic characterization by MS. Data were collected from three distinct biological preparations after FFE separation of plant Golgi membranes. The three independent separations produced very similar A_{280} profiles to those outlined previously (Fig. 2). To precisely determine the purified Golgi fractions after FFE analysis, fractions from the Golgi-enriched region (typically fractions 15–25) were each concentrated by ultracentrifugation and analyzed by LC-MS/MS (data not shown). Marker proteins from previous organelle proteomic surveys were used to identify the contiguous fractions (usually two to three) that contained a significant enrichment of Golgi proteins with minimal contaminants. Each fraction enriched for Golgi markers was selected for further in-depth analysis by LC-MS/MS and interrogated against The Arabidopsis Information Resource (TAIR) release 10 protein data set (Supplemental Table S1). The contributions of each biological replicate analyzed by LC-MS/MS were as

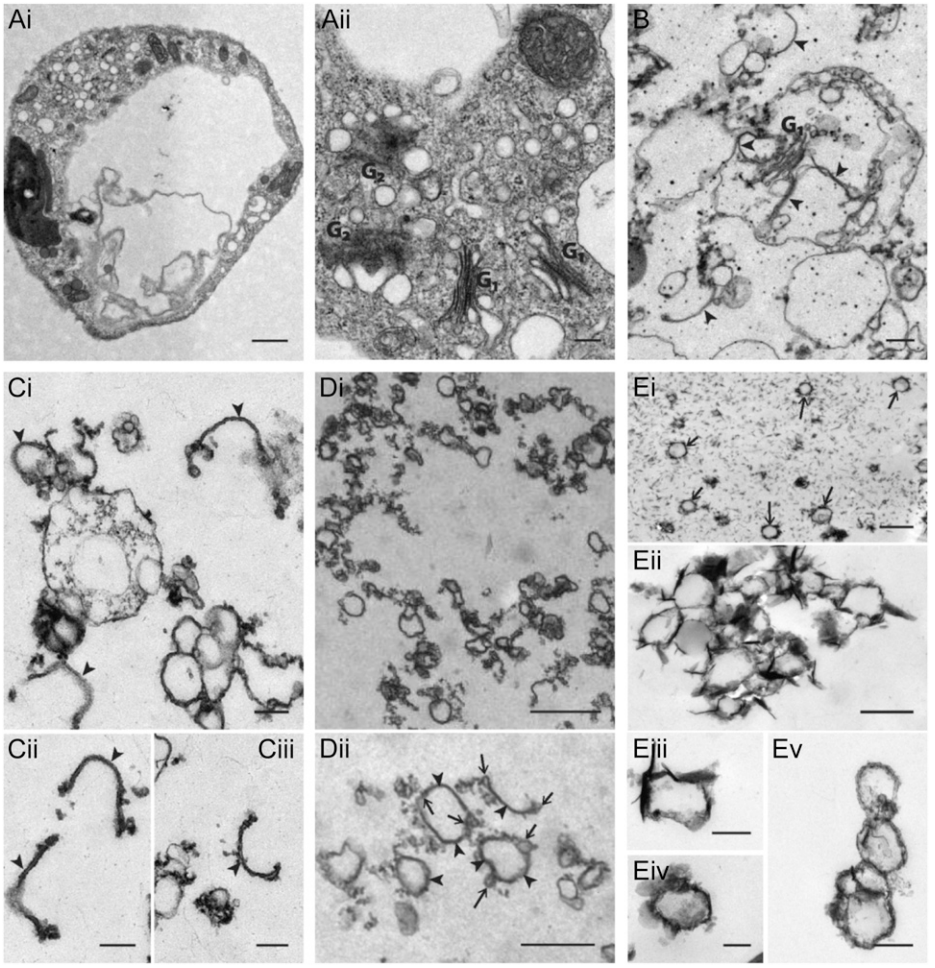

Figure 3. Morphological analysis by electron microscopy of the sequential purification of Golgi membranes from Arabidopsis. A, Whole protoplasts in which intact Golgi stacks are visible in cross-section (G1 [Ai]) and tangential section (G2 [Aii]). B, Homogenate in which both individual cisternae (arrowheads) and loosely intact Golgi stacks (G1) were seen. C, The homogenate after centrifugation at 50,000*g* onto a 1.6 M Suc layer in which structures reassembling individual cisternae (arrowheads) were seen. D, The interface collected after centrifugation at 100,000*g*, which was analyzed by FFE (overview [Di]). This contained numerous densely staining membrane structures in rings or arcs (arrowheads [Dii]) with small, bulbous swelling at the periphery (arrows [Dii]). E, Post-FFE fractions containing purified Golgi contained homogenous vesicular structures (arrows [Ei]) of approximately 200 to 400 nm diameter (Eii–Ev). A combination of buffers used for transmission electron microscopy, FFE, and density centrifugation most likely caused the crystal-like formations. Bars = 1 μm (Ai, Di, and Ei), 500 nm (Eii), 200 nm (Aii, B, Ci–Ciii, Dii, and Ev), and 100 nm (Eiii and Eiv).

follows: AtGolgi-1 (594 proteins), AtGolgi-2 (449 proteins), and AtGolgi-3 (508 proteins), which excluded redundant protein matches (Supplemental Fig. S2). Combining all three analyses, a total of 778 distinct proteins were identified. Protein matches (including redundant matched proteins) were required to have been identified in at least two replicates with a distinct identification in one replicate to be assigned with confidence to the final proteome. This resulted in a set of 491 proteins and defined a reproducible Arabidopsis Golgi proteome (Supplemental Table S2). Proteins that had fulfilled the above criteria but were not unambiguously identified in at least one preparation were removed (i.e. proteins spanning the same set of peptides). Although excluded from the final set, these proteins still represent potentially valid identifications, although most are derived from alternate splice transcripts (Supplemental Table S3).

Defining the Arabidopsis Golgi Proteome

In an attempt to further define the 491 proteins comprising the reproducible Arabidopsis Golgi proteome, we exploited the extensive subcellular proteomics that has already been undertaken in Arabidopsis (Heazlewood et al., 2007). Using these data, it was possible to directly assign contaminants based on extensive experimental localization data. A total of 64 proteins were assigned as organelle contaminants using this approach, with a further 56 assigned to the protein synthesis classification based on experimental annotations (Supplemental Table S2). Specific organelle contaminants comprised mitochondrion (28 proteins), the ER (15 proteins), the cytosol (14 proteins), and six proteins from the plastid, nucleus, and peroxisome, collectively. Using quantitative spectral counting techniques, the relative contribution of contaminants was estimated at 13% of the identified proteome and protein synthesis proteins at 6% (Fig. 4). Functional analysis of the remaining 371 proteins showed a significant proportion of proteins with no distinct functional role (13% not assigned), suggesting further diverse roles for the Golgi apparatus. Significantly, the largest functional group was proteins involved in sugar metabolism (20%), a major function of the plant Golgi apparatus. This group includes over 50 GT and GT-like proteins, many of which have been determined to be involved in matrix polysaccharide biosynthesis. This was followed by transporters and

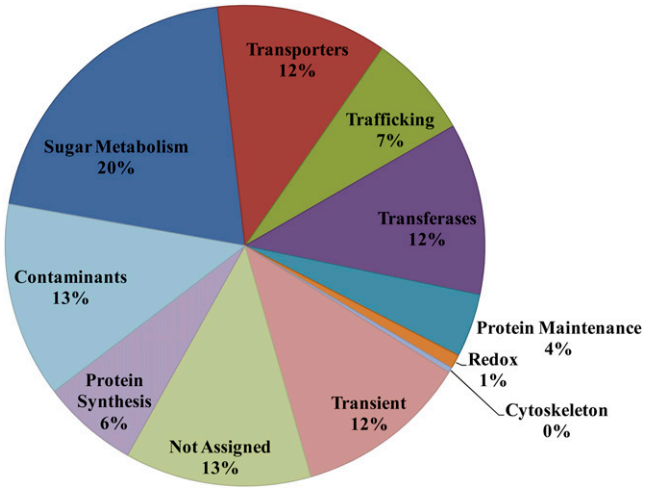

Figure 4. Broad functional classification of the Arabidopsis Golgi proteome. Proteins were assigned functional categories based on published information, experimental subcellular localizations (Heazlewood et al., 2007), MapMan categories (Thimm et al., 2004), and functional domains (Supplemental Table S2). Relative proportions of each functional group were determined using average spectral counts from the three Golgi replicates. The largest category represents proteins involved in sugar metabolism (e.g. GTs) followed by proteins with little functional information (not assigned). Proteins likely to be transiting through the Golgi (transient) were determined using experimental localization information derived from post-Golgi membrane systems (e.g. plasma membrane, extracellular, or vacuole).

associated proteins (12%), transferases (12%), trafficking proteins (7%), and a group involved in protein maintenance functions (5%). Of the 371 proteins identified in the Golgi proteome, a total of 78 (21%) had been previously localized to the Golgi or endomembrane by either proteomics or fluorescent protein localization. When dealing with a secretory pathway, it is important, but sometimes difficult, to distinguish transitory proteins destined for elsewhere from functionally active, resident proteins. Abundant experimental evidence exists for the vacuolar, extracellular, and plasma membrane localization of a proportion of proteins identified in this study (Heazlewood et al., 2007). Within the set of 371 proteins, proteins were classified as transitory based on whether they had been repeatedly identified in the vacuole, plasma membrane, or extracellularly. Proteins with multiple demonstrated locations, such as members of the cellulose synthase (CESA; Persson et al., 2007) or vacuolar ATP synthase (V-ATPase) complex (Sze et al., 2002), were excluded. This provided strong evidence that 55 proteins, or 12% of total proteins, were in transit through the Golgi apparatus (Fig. 4; Supplemental Table S2).

Assessment and Validation of the Golgi Proteome

We attempted to correlate the distribution of proteins presented in this study with distribution patterns shown by known Golgi markers during FFE, so that a confidence rank for Golgi localization could be assigned to each of the 491 proteins (Supplemental Fig. S3). This way, Golgi localization versus contamination could be assessed per protein, a more useful approach than assigning all proteins of uncertain location to the Golgi using a single confidence bracket. Two further independent Golgi preparations were undertaken to produce the necessary resolution for the proteomic analysis of fractions for confidence assignments. A total of 22 post-FFE fractions were individually analyzed by LC-MS/MS, covering FFE fractions 13 to 43. Different abundance profiles of each protein over the fractions provided an estimate of similarity when compared with the distribution profiles of Golgi markers or known contaminants. Based on this analysis, a Golgi marker correlation rank was developed indicating low confidence (1) or high confidence (5). Only 37 of the 491 proteins reproducibly identified in the proteomic characterization of AtGolgi-1, AtGolgi-2, and AtGolgi-3 (Supplemental Table S2) were unable to be allocated a confidence rank due to poor representation in these new analyses. Significantly, 12 of these 37 proteins were previously allocated as contaminants, further highlighting the reproducibility of this approach. Low-scoring proteins in this set include many non-Golgi proteins (e.g. HSP70), while several of the highest scoring proteins have documented functions in the Golgi (e.g. XXT5 or MUR2; Supplemental Fig. S3C). While these scores are helpful in assessing likely Golgi localization for a particular protein, it is worth noting that this 371-protein data set is derived from fractions already highly enriched in Golgi and a lower score is not necessarily indicative of contamination; UXS4 has been previously localized to the Golgi (Dunkley et al., 2006) but receives a low confidence rank of 2 (Supplemental Fig. S3C; Supplemental Table S2) compared with nontransitory proposed Golgi proteins (average rank score of 3.43).

The success of the FFE approach for the purification of Golgi was further examined by confirming the localization of a collection of proteins using C-terminal yellow fluorescent protein (YFP) fusions. A total of 14 proteins were selected that had been allocated to the Golgi proteome in this study. The selected proteins had a range of confidence values, protein scores, and various subcellular assignments by MS (Supplemental Table S2). Transient transformation assays were undertaken, and after overnight incubation, 13 of the YFP constructs resulted in signals corresponding to punctate structures within the cell (Fig. 5). A cotransformed Golgi marker (GmMan1::cyan fluorescent protein [CFP]) confirmed the cis-Golgi identity of these punctate structures. A Golgi-ER localization signal was also observed for three proteins, ACC oxidase 2 (AT1G62380.1; Fig. 5C), a putative nucleotide sugar transporter (AT3G11320.1; Fig. 5E), and an HRF1 protein (AT3G59500.1; Fig. 5G), and could indicate multiple localizations of these proteins in the secretory system. Significantly, a dehydration stress protein (At1g32090.1;

Fig. 5B) allocated as a transient protein in the Golgi proteome was localized to the plasma membrane, confirming its presence in the Golgi as a transient or cargo protein. Finally, of the 93 proteins previously allocated to the Golgi by MS (Dunkley et al., 2006), 78 (84%) were identified in this proteome. The exceptionally high overlap of proteins assigned to the Golgi in these studies, together with the other validation techniques outlined above, support the quality of the FFE purification process in isolating high-purity Golgi membranes from plants.

Functional Characterization of a Golgi NDPase

To highlight the potential functional significance of this data set, we selected a candidate that had been extensively characterized in roles unrelated to functions within the plant Golgi apparatus. The ATAPY1 protein (AT3G04080.1) is reported to be a member of the plant apyrase family and to function as an ectoapyrase at the plasma membrane (Wu et al., 2007). Previous work using recombinant ATAPY1 has indicated that the enzyme functions as an apyrase and is capable of hydrolyzing both ATP and ADP (Steinebrunner et al., 2000). The Golgi localization of ATAPY1 was confirmed using a YFP marker (Fig. 5D). These previous activity data together with the confirmed subcellular information indicated that ATAPY1 may function as an NDPase, converting nucleoside diphosphates formed after glycosylation reactions to nucleotides within the Golgi apparatus. To ascertain whether ATAPY1 could function as an NDPase in vivo, a complementation assay was undertaken. The *Saccharomyces cerevisiae* mutant Δ*gda1* lacks the Golgi guanosine diphosphatase gene (*GDA1*) and results in the partial loss of *O*- and *N*-glycosylation of proteins (Abeijon et al., 1993). The *ATAPY1* gene was transformed into the Δ*gda1* and wild-type backgrounds to determine whether it could functionally complement

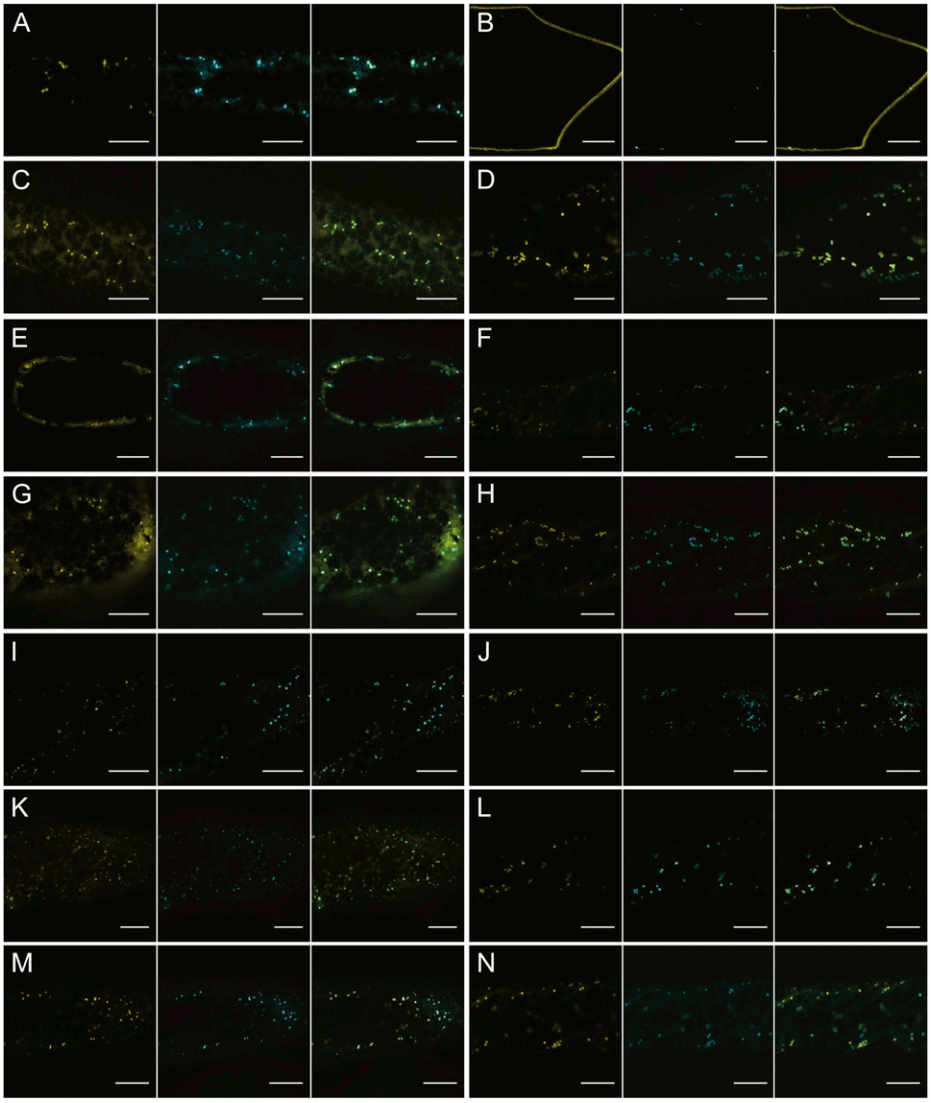

Figure 5. Confirmed subcellular localization of selected proteins by C-terminal YFP fusions. The C-terminal YFP constructs were colocalized using the cis-Golgi marker construct *GmMan1*::*CFP*. For each set of three panels, the first panel contains the protein of interest as a YFP construct (yellow), the second panel shows the signal from the cotransformed *GmMan1*::*CFP* (cyan), and the third panel shows the merged image of the YFP and CFP signals. A, AT1G27200.1, DUF23/GT0. B, AT1G32090.1, dehydration stress protein (ERD4). C, AT1G62380.1, ACC oxidase 2. D, AT3G04080.1, apyrase 1. E, AT3G11320.1, nucleotide-sugar transporter. F, AT3G23820.1, UDP-D-glucuronate 4-epimerase 6. G, AT3G59500.1, HRF1 protein. H, AT4G27720.1, major facilitator protein. I, AT4G30440.1, UDP-D-glucuronate 4-epimerase 1. J, AT4G33910.1, oxygenase protein. K, AT5G18280.1, apyrase 2. L, AT5G20350.1, ankyrin protein. M, AT5G36290.1, uncharacterized protein. N, AT5G58970.1, uncoupling protein 2 (UCP2). Bars = 10 μm.

the reduced glycosylation phenotype by detecting the recovery of protein glycosylation through immunoblotting (Herrero et al., 2002). The effect of the Δ*gda1* mutant on the mobility of the carboxypeptidase Y protein by SDS-PAGE compared with the wild type confirmed the reduced glycosylation in this mutant (Fig. 6). Transformation of the Δ*gda1* mutant with the *ATAPY1* gene construct successfully complemented the reduced glycosylation phenotype (Fig. 6). These results confirm the ability of the ATAPY1 product to function as an NDPase in the secretory system of *S. cerevisiae*.

DISCUSSION

This study outlines, to our knowledge, the first high-purity isolation and proteomic characterization of the Golgi apparatus from plants. In recent years, it has been demonstrated that organelle enrichment and subsequent purification by FFE is a powerful combination in the characterization of subcellular proteomes (Eubel et al., 2008; Huang et al., 2009). Here, to our knowledge for the first time, such approaches have been employed in the isolation of Golgi membranes from a complex background of contaminants with similar densities and surface charges. A Golgi proteome of 371 proteins, excluding contaminants and protein synthesis proteins, has been proposed, representing a sizable increase in Golgi-localized proteins; SUBA (Heazlewood et al., 2007) lists 173 proteins as experimentally localized to the Golgi. This proteome includes important regulatory and biosynthetic proteins in the secretory pathway of plants as well as many unknown proteins and, therefore, appreciably expands our potential for understanding Golgi-localized processes.

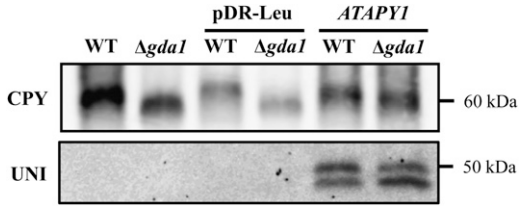

Figure 6. Functional characterization of *ATAPY1* with the *S. cerevisiae* Δ*gda1* mutant. An antibody against the carboxypeptidase Y protein (CPY) was used to assess protein glycosylation in the Δ*gda1* mutant. The empty expression vector (pDR-Leu) was employed as a control for complementation by the pDR-Leu-*ATAPY1* (*ATAPY1*) construct. A recovery in CPY glycosylation (vertical migration) is observed in the Δ*gda1* mutant expressing the ATAPY1 protein. The slight vertical deviation of complemented CPY may reflect issues in migration in SDS-PAGE that can occur with glycoproteins or could indicate that incomplete or partial glycosylation has occurred. Confirmation of ATAPY1 expression was assessed using the universal antibody (UNI) against a Gateway-specific epitope at the C terminus of the construct. The observed doublet could represent processing or a modification of the ATAPY1 protein. WT, Wild type.

Untangling the Endomembrane

The Golgi apparatus represents the central hub of the protein secretory pathway, with proteins destined for the plasma membrane, vacuole, and extracellular regions passing or cycling through this organelle. Defining the functional Golgi proteome, therefore, requires extensive information about the role of the organelle within the cell. While transitory proteins could be classified as contaminants, it is difficult to distinguish between transiting and nonfunctional proteins and those undertaking a functional role. The secretory system highlights the inherent difficulties in attempting to apply broad subcellular classifications to a complex and fluid biological system.

Some protein complexes colocalize to the Golgi and other compartments: the V-ATPase complex features prominently in vacuolar proteomes (Carter et al., 2004) but is localized throughout the endomembrane system (Sze et al., 2002) and is functionally involved in the acidification of Golgi-derived secretory vessels (Strompen et al., 2005). Proteins of all eight peripheral V_1 subunits of the V-ATPase complex were highly prominent in our proteomic analysis (Supplemental Table S2). The CESA complex also exhibits dual localization, cycling between the Golgi and plasma membrane, where it synthesizes cell wall cellulose (Paredez et al., 2006). The CESA complex consists of three subunits (Desprez et al., 2007; Persson et al., 2007), of which CESA1 (AT4G32410.1) and CESA3 (AT5G05170.1) were consistently identified in this proteome (Supplemental Table S2).

Identifying ER versus Golgi proteins raises colocalization and functionality questions, as these two membrane systems are highly connected in plants (Boevink et al., 1998). Isoforms of calreticulin (CRT1 [AT1G56340.1] and CRT2 [AT1G09210.1]), binding immunoglobulin proteins (BiP [AT5G28540.1] and BiP2 [AT5G42020.1]), and eight members of the protein disulfide isomerase family (PDI/PDIL) were identified in this study (Supplemental Table S2). BiP, CRT, and members of the PDI/PDIL family are frequently referred to as ER-lumen resident protein chaperones (Galat and Metcalfe, 1995; Jelitto-Van Dooren et al., 1999; Frand et al., 2000; Wu et al., 2010a). For a number of years, the definition of these proteins as ER residents has been questioned (Turano et al., 2002), and while BiP, CRT, and several of the PDI members identified in this study have been localized by fluorescent protein to the ER (Eubel et al., 2008; Wang et al., 2008), it is interesting that localization by MS suggests a more ubiquitous distribution (Heazlewood et al., 2004; Jaquinod et al., 2007; Marmagne et al., 2007; Mitra et al., 2009). It has now been conclusively demonstrated that BiP and CRT cycle between the ER and cis-Golgi and that both BiP and PDI1-1 are transported to lytic vacuoles via the Golgi apparatus (Pimpl et al., 2006; Ondzighi et al., 2008). The lack of the vesicular coat protein complex (COPI and COPII) components is intriguing, given their roles in ER-to-Golgi shuttling (Robinson et al.,

2007). A recent analysis of the Arabidopsis cytosolic proteome (Ito et al., 2011) consistently identified members of both COPI and COPII complexes. These observations suggest that the COP complexes are loosely bound to the Golgi apparatus and hence absent in this Golgi proteome.

By comparison, the identification of major vacuolar and plasma membrane components transiting the Golgi is less challenging. In recent years, extensive proteomic surveys using improved purification strategies have been undertaken in Arabidopsis (Jaquinod et al., 2007; Mitra et al., 2009). These and other studies have identified nearly 800 proteins from the tonoplast and over 3,000 proteins from the plasma membrane (Heazlewood et al., 2007). Exploiting these data enabled organelle profiling of Golgi-enriched FFE fractions. Analysis of fractions adjacent to those used for the proposed proteome showed more cathodic trends for both tonoplastic and plasma membrane proteins compared with Golgi markers. Therefore, plasma membrane and/or tonoplastic proteins comigrating with the most Golgi-enriched fractions are likely to be in transit through the Golgi. Previous studies concerning the migration of vacuolar and plasma membrane fractions from plants during FFE have found vesicles that migrated to anodic and cathodic extremes, respectively (Canut et al., 1988, 1990; Barkla et al., 2007). The discrepancy in vacuolar migration between this and earlier studies may be because MS was not used and analyses were based on limited markers, such as enzyme activities or antibodies, which potentially could not have distinguished prevacuolar compartments, lytic vacuoles, the trans-Golgi network, or the central vacuole. Equally, though, without specific preenrichment for either the vacuole or tonoplast vesicles, the migration of either during FFE cannot be fully described here. The migration of plasma membrane vesicles, defined here with numerous markers, is in agreement with previous findings (Canut et al., 1988, 1990), supporting the transitory identity of plasma membrane proteins comigrating with the Golgi.

A quantitative assessment of this proteome by spectral counting puts proteins involved in protein synthesis at approximately 6% (Fig. 4). Proportionally, this is similar to studies in which ribosomal contamination has been minimized through the addition of protein biosynthesis inhibitors such as cycloheximide (Wu et al., 2004). Ribosomal and associated proteins are well annotated and therefore can be easily identified and removed from the proteome. The effect of inhibiting translation on Golgi structure and integrity is unknown, but since structural preservation was important to the successful electrophoretic migration, the addition of protein biosynthesis inhibitors was not attempted.

GTs and Cell Wall Composition

The sugar metabolism category comprised GTs, glycosyl hydrolases, and nucleotide-sugar interconverting enzymes and accounted for 20% of the proteins assigned to the Golgi proteome (Supplemental Table S2). As these data were taken from undifferentiated cell cultures, they were enriched for GTs involved in primary cell wall synthesis. While the experimental system used will have affected the GTs expressed, many of the key GTs identified from Arabidopsis plants were present (Supplemental Table S4). Therefore, proteins involved in cell wall biosynthesis using this experimental system can be an important reference for future research into primary cell wall synthesis in dicots.

Although only one glucan synthase is theoretically required for xyloglucan synthesis, two glucan synthases, CSLC04 (AT3G28180.1) and CSLC06 (AT3G07330.1), were identified consistently in all three experiments. Only CSLC04 has been examined and assigned a function in xyloglucan biosynthesis (Cocuron et al., 2007). Given the consistent presence of CSLC06 in this study, it would make a worthy target for further study. Callose deposition by glucan synthase-like (GSL) proteins is an important component of cell plate formation during cytokinesis (Chen et al., 2009). The presence of GSL05 (AT4G03550.1), GSL08 (AT2G36850.1), and GSL10 (AT3G07160.1) in all experiments was likely influenced by the rapid cell division induced in these cells in the presence of exogenous kinetin.

A clear link has been shown between the abundance of arabinan linkages and the undifferentiated state of suspension-cultured cells (Willats et al., 1999). Arabinan structures are complex, and their synthesis theoretically requires several GTs. Therefore, multiple arabinosyltransferases could be expected in this proteome. A plausible arabinosyltransferase, ARAD1 (AT2G35100.1; Harholt et al., 2006), was identified in this work along with its homolog, AT5G16890.1 (Supplemental Table S4).

The homopolymer forming the pectic backbone, homogalacturonan, is synthesized by galacturonosyltransferases (GAUTs) in family GT8 (Sterling et al., 2006; Caffall et al., 2009). GAUT1, -4, -7, -8, -9, and -10 were present in all preparations, with GAUT3 and -11 present in two. Many GAUTs were identified here, so complete redundancy in homogalacturonan synthesis seems unlikely. It is possible that some of these proteins form complexes requiring at least two family members (Mohnen, 2008), or GAUTs required for the synthesis of the GalUA backbone may vary according to the final structure.

Carbohydrate modification of proteins destined for both the cell wall and other subcellular locations occurs in the Golgi (Saint-Jore-Dupas et al., 2006). The PGSIP2 (GUX3) protein is a close homolog of the PGSIP1 (GUX1) and PGSIP3 (GUX2) proteins, which have recently been shown to be glucuronosyltransferases responsible for adding GlcA residues to the xylan backbone (Mortimer et al., 2010; Oikawa et al., 2010). GUX1 and GUX2 are highly expressed in cells with secondary wall growth, unlike GUX3, which was found in this study, and likely to add GlcA to xylan in

primary walls. PGSIP6 is more distantly related to GUX1, -2, and -3 (Yin et al., 2010) and was also found in our Golgi proteome.

The glycosylation of proteins destined for the cell wall and elsewhere occurs in the Golgi (Saint-Jore-Dupas et al., 2006). Of the 44 GTs identified in this study, 16 were either known or predicted to be involved in protein glycosylation (Supplemental Table S2). The proteins GNT1 (AT4G38240.1), XYLT (AT5G55500.1), and FUT12 (AT1G49710.1) in this proteome are involved in the main *N*-glycosylation pathway (Strasser, 2009). GALT1, a member of this core pathway, was not identified, but two other members of the same family, GT31, were (AT1G53290.1 and AT2G26100.1; Supplemental Table S2). Significantly, no ER-localized GTs involved in the *N*-glycosylation pathway were observed (Strasser, 2009). However, several non-GT glycotransferase components implicated in *N*-linked glycosylation were identified, including members of the oligosaccharyltransferase ER complex Ribophorin I (AT1G76400.1), HAP6 (AT4G21150.1), and DGL1 (AT5G66680.1), which are involved in the transfer of preassembled oligosaccharides to proteins (Kang et al., 2008). Other GTs potentially involved in protein glycosylation include members of the GT14 family (AT5G39990.1, AT3G24040.1, and AT1G71070.1) and DUF266 proteins (AT1G11940.1 and AT5G11730.1). These proteins contain functional domains implicated in side chain branch formation in *O*-linked glycans (Yeh et al., 1999) and may reflect the Golgi-localized modifications of arabinogalactan proteins destined for the cell wall (Zhou et al., 2009). Finally, although the GT65 family is involved in the *O*-fucosylation of proteins (Wang et al., 2001), only one protein from Arabidopsis is currently allocated to this family at the Carbohydrate-Active EnZymes database (Cantarel et al., 2009). This particular protein was not identified here, but nine proteins sharing the same Pfam domain (PF10250) were found (GT-like). A recent bioinformatics analysis looking to uncover further novel Arabidopsis GTs identified three proteins with a similar domain, one of which was found in this study (Hansen et al., 2009), while six have already been localized to the Golgi (Dunkley et al., 2006). Domain annotation is based on mammalian data and so cannot be used to interpret function in plants. *O*-Fucosylation of arabinogalactan proteins has recently been shown to involve members of the GT37 family (Wu et al., 2010b).

NDPases of the Plant Golgi

The biosynthesis of matrix polysaccharides and protein glycosylation by GTs within the Golgi apparatus require energetic donors in the form of nucleotide sugars. After glycosylation reactions, nucleoside diphosphates are liberated and subsequently converted to nucleotides by NDPase and are thought to exit the Golgi lumen through the action of nucleotide sugar-exchange transporters (Reyes and Orellana, 2008). Although NDPase activity assays have been employed to assess Golgi membrane enrichment in plants for decades (Fig. 1), the actual proteins responsible for these reactions have remained unknown. During the analysis of the Golgi proteome, we identified the previously reported, plasma membrane-localized ectoapyrases ATAPY1 (AT3G04080.1) and ATAPY2 (AT5G18280.1; Wu et al., 2007). The consistent identification across replicates and the previous biochemical characterization of these proteins as phosphatases of both ATP and ADP (Steinebrunner et al., 2000) indicated that they may represent the as yet uncharacterized Golgi-resident NDPases. The colocalization of both the ATAPY1 and ATAPY2 proteins with the CFP fluorescent marker to the Golgi apparatus (Fig. 5) and the subsequent functional complementation of the *S. cerevisiae* GDPase mutant Δ*gda1* with ATAPY1 confirmed both the subcellular location and the functional role of these enzymes in plants (Fig. 6). Both ATAPY2 and ATAPY1 proteins share high sequence identity (Steinebrunner et al., 2000), indicating that ATAPY2 may also function as a Golgi-resident NDPase. The expression of both *ATAPY1* and *ATAPY2* is fairly ubiquitous throughout the plant, with increased expression associated with dividing cells, an expression pattern consistent with their roles as NDPases (Wolf et al., 2007; Wu et al., 2007).

CONCLUSION

This study outlines, to our knowledge, the first isolation and proteomic characterization of high-purity Golgi membranes from plants and marks a significant advancement on previous isolation strategies. This analysis of Golgi membranes will be a hugely important resource enabling the prioritization of research into both known and uncharacterized Golgi proteins. Thus far, many hundreds of proteins have been predicted to act as GTs, and this study provides an opportunity to assess the relative importance of some of these putative GTs in primary cell wall synthesis. Finally, the value of this Golgi proteome was demonstrated through confirmed localization and functional characterization of a plant Golgi NDPase (ATAPY1) that had been previously reported to function at the plasma membrane in nucleotide signaling. This proteomic characterization of the Golgi is a timely addition to plant cell wall science, where the advent of biofuels-related research demands a rapid expansion of the current knowledge base.

MATERIALS AND METHODS

Plant Material

Arabidopsis (*Arabidopsis thaliana* Landsberg *erecta*) cell suspension cultures (100 mL) were grown at 22°C under constant moderate light and shaking (125

rpm) in 1× Murashige and Skoog basal salt medium (Phyto Technology Laboratories) supplemented with 2% Glc (w/v), α-naphthaleneacetic acid (0.5 mg L^{-1}), and kinetin (0.05 mg L^{-1}) and adjusted to pH 5.8 with 1 M KOH. Cells (10 mL) were inoculated weekly into fresh medium.

Construct Generation

Coding sequences were amplified from cDNA derived from Arabidopsis cell cultures using specific primers (Supplemental Table S5). PCR products were recombined into pDONR221-f1 (Lalonde et al., 2010) according to the manufacturer's instructions (Life Technologies) and verified by sequencing.

Transient Transformation and Fluorescence Microscopy

The pDONR221-f1 constructs were recombined into pBullet GW-YFP G-CFP, a customized bombardment vector containing a Gateway recombination site fused to a C-terminal YFP, and *GmMan1*::*CFP*, the α-ManI cis-Golgi marker from *Glycine max* (Nelson et al., 2007). DNA was prepared from liquid cultures with either the Qiagen Midiprep Plus kit or the Promega PureYield Midiprep system. After 1 h at 22°C on agar containing 2% Suc and 0.5× Murashige and Skoog medium, onion (*Allium cepa*) peels were bombarded using a PDS-1000 particle bombardment system (Bio-Rad). Plasmid DNA (1–5 μg) was used to coat 50 μL of gold particles (1 μm, 60 mg mL^{-1}; Bio-Rad) in the presence of 20 mM $CaCl_2$ and 0.8 mM spermidine for 3 min with mild vortexing. Particles ethanol dehydrated onto macrocarrier discs were accelerated into onion peels by helium bursts at 1,100 ψ under 28 inches of mercury vacuum. Bombarded onions were dark incubated at 22°C for 18 to 22 h before confocal microscopy. Transformed samples were analyzed using a Zeiss LSM710 meta (QUASAR detector) equipped with a 408-nm diode, argon, and In Tune laser. Images were taken using the inverted scope with a 1.30 numerical aperture oil 40× objective. For colocalization experiments, samples tagged with CFP and YFP were fixed with formaldehyde and imaged sequentially using excitation/emission of 405 nm/454 to 515 nm for CFP and 514 nm/519 to 621 nm for YFP. Detector gain was 622, with a pixel dwell time of 1.15 μs. The Zen software package (Carl Zeiss) was used for image acquisition, while ImageJ (version 1.44) was used for image analysis and processing (Abramoff et al., 2004).

Complementation Analysis

The *ATAPY1* (AT3G04080.1) pDONR221-f1 construct was recombined into a Gateway-modified pDR-Leu vector generated by transferring the pPMA-GW-tADH expression cassette from pDRf1-GW into the YEplac181 shuttle vector (Gietz and Sugino, 1988; Rentsch et al., 1995; Loqué et al., 2007) for use in complementation analysis. The pDR-Leu empty vector and the pDR-Leu containing *ATAPY1* were transformed into *Saccharomyces cerevisiae* strains BY4741 (wild type: *MATa*, *his3Δ1*, *leu2Δ0*, *met15Δ0*, *ura3Δ0*) and Δ*gda1* (*MATa*, *his3Δ1*, *leu2Δ0*, *met15Δ0*, *ura3Δ0*, *gda1Δ0*) using standard methods (Gietz and Woods, 2002). Transformed *S. cerevisiae* lines were cultured for protein extraction and further analysis as described (Eudes et al., 2011).

Golgi Isolation and Enrichment

Protoplasts prepared from 7-d-old cells according to previous methods (Meyer and Millar, 2008) were resuspended in 0.4 M Suc in buffer A (10 mM Na_2HPO_4, 3 mM EDTA, 2 mM dithiothreitol, 0.1% bovine serum albumin [w/v], and 1% dextran 200000 [w/v]) in a 1:1 (w/v) ratio, based on cell fresh weight, and ruptured in a Potter-Elvehjem homogenizer. The homogenate was centrifuged at 5,000*g* for 15 min at 4°C, and the supernatant was cushioned onto 1.6 M Suc in buffer A at 50,000*g* for 1 h at 4°C. The supernatant was replaced with cold 1.0 M Suc (20 mL) in buffer A and overlaid with cold 0.75 M Suc in buffer A (without bovine serum albumin) and cold 0.2 M Suc (Tris-HCl, pH 7.4). After centrifugation at 100,000*g* for 1.5 h at 4°C, membranes were collected from the 0.75/1.0 M Suc interface. Protein concentration was adjusted to 5 μg mL^{-1}.

Separation by FFE

FFE (Becton-Dickenson) was performed using a separation chamber height of 0.5 mm. All FFE buffers were prepared as reported previously (Eubel et al., 2007) but adjusted to pH 7.1 (separation and counter flow buffers) or pH 6.5 (stabilization and circuit buffers) with 1 M NaOH. A voltage of 640 to 680 V was applied, which resulted in a current of 120 to 125 mA. Sample injection speed was 2,000 μL h^{-1}. Fractions were collected on precooled 2-mL 96-well plates. The separation chamber was cooled to 5°C. Membranes were collected from fractions by centrifugation at 50,000*g* for 45 min at 4°C and resuspended in cold 10 mM Tris-HCl, pH 7.5.

Organelle Marker Protein Selection

Proteins were chosen as organelle markers according to the certainty with which they had been experimentally localized, using data from SUBA (Heazlewood et al., 2007). Proteins were classified as transitory based on whether they had been identified in the vacuole, plasma membrane, or extracellularly by four independent proteomics studies (MS) or fluorescent protein analysis. Markers for contaminating organelles (mitochondria, peroxisome, nucleus, and plastid) were defined as having a majority of experimental localizations to the organelle in question. As less proteomic data were available for cytosolic, ER, or Golgi proteins, markers for these organelles were defined by an equal number of localizations both to these organelles and to other locations, as a minimum requirement.

NDPase Assay

Samples were concentrated after FFE by centrifugation at 100,000*g* prior to analysis and repeatedly frozen/thawed prior to analysis. The assay was conducted using the Malachite Green Phosphate Assay (ScienCell Research Laboratories) according to the manufacturer's instructions using a total of 20 μg of protein and reaction procedures outlined by Schaller and DeWitt (1995).

Gel Electrophoresis and Immunoblotting

Protein (5 μg) from FFE fractions was separated by 8% to 16% SDS-PAGE and transferred to nitrocellulose membranes according to Ito et al. (2011). Protein (5 μg) from *S. cerevisiae* cultures was separated by 10% SDS-PAGE and transferred to nitrocellulose according to Ito et al. (2011). Antibodies were obtained from Abcam (CRT1, calreticulin [ab2907]; CPY, carboxypeptidase Y [ab34636]) and Agrisera (PsbA, AS05084; VDAC1, AS07212; cFBPase, AS04043). All procedures and dilutions were undertaken according to instructions by the manufacturers. The α-ManI antibody, a gift from Dr S. Bednarek (University of Wisconsin, Madison), was used at a 1:4,000 dilution. The universal antibody against the Gateway attB2 site (Invitrogen) was used at a 1:15,000 dilution (Eudes et al., 2011). Detection was conducted using the peroxidase-linked secondary antibody anti-rabbit IgG (Sigma-Aldrich) with SuperSignal West Dura Extended Duration Substrate (Thermo Fisher Scientific) and recorded on a BioSpectrumAC Imaging System (UVP).

Electron Microscopy

Samples were fixed immediately in glutaraldehyde at a final concentration of 2.5%, mixed with 2% agarose, cooled, stained with 2% OsO_4 for 1 h, and washed twice in buffer A (see above). Samples were stained with uranyl acetate for 1 h and cold dehydrated in an ethanol series. Samples were washed twice in 100% acetone, transferred to an Epon Araldyte-acetone series, and embedded in Epon Araldyte resin. Sections (80 nm) were cut on a Leica Ultramicrotome and stained with uranyl acetate (2%) and Reynolds lead citrate. Ultrastructural observations were performed with an electron microscope (FEI Tecnai 12) operating at 120 kV and equipped with a 2kx2k CCD camera.

Quadrupole Time-of-Flight MS

All samples for MS were digested with trypsin (1:10, w/w) overnight in 40% methanol. Peptides were purified and concentrated using C18 Ultra-Micro TipColumns (Harvard Apparatus). For analysis of FFE-separated samples by LC-MS/MS, samples (1 μg) were analyzed by electrospray ionization quadrupole time-of-flight (Q-TOF) mass spectrometer (QSTAR Elite Hybrid Quadrupole TOF; AB Sciex) using a Eksigent nano-LC system (AB Sciex) incorporating a 75-μm × 15-cm PepMap C_{18} reverse-phase column (Dionex) at a flow rate of 300 nL min^{-1}. Peptides were analyzed by MS over a 150-min gradient using buffers A (2% acetonitrile [v/v], 0.1% formic

acid [v/v]) and B (98% acetonitrile [v/v], 0.1% formic acid [v/v]). Three product ion scans were collected from each cycle with a maximum 2-s accumulation time depending on the intensities of fragment ions. A threshold of 50 counts was required for ions to be selected for fragmentation. Parent ions and their isotopes were excluded from further selection for 1 min with a mass tolerance of 100 ppm.

MS Data Analysis

Data were exported as .mgf files from Analyst QS version 1.1 using the script available from Matrix Sciences (version 1.6b23). The export settings were as follows: centroid the survey scan ions (TOF MS) at a height percentage of 50% and a merge distance of 0.1 atomic mass unit (for charge-state determination); centroid MS/MS data at a height percentage of 50% and a merge distance of 2 atomic mass units; reject a collision-induced dissociation if it contained fewer than 10 peaks; and discard ions with charge states greater than or equal to 5. Multiple fractions from FFE-separated samples were analyzed by LC-MS/MS from each independent Golgi preparation (total of three). The purified Golgi fractions were determined by initially profiling approximately 10 post-FFE fractions by LC-MS/MS. Highly purified Golgi fractions determined by the presence or absence of organelle markers were each subjected to in-depth characterization by LC-MS/MS. All MS/MS data from each highly purified Golgi post-FFE fraction (total of two to three) were merged into a single data file (.mgf) for each preparation, namely AtGolgi-1 (FFE fractions 20 and 21), AtGolgi-2 (FFE fractions 20–22), and AtGolgi-3 (FFE fractions 20 and 21). Prior to database interrogation, parent spectra were calibrated using the DtaRefinery utility (version 1.2; Petyuk et al., 2010). Briefly, .mgf data files were converted to .dta data files and used to query the latest Arabidopsis protein set (TAIR10, comprising 35,393 sequences and 14,486,052 residues) by DtaRefinery, which employs X!Tandem (0.01 maximum valid expectation value, ±200 ppm parent monoisotopic mass error tolerance, and dynamic posttranslational modifications: oxidation (M). Recalibration of parent ions employed additive regressions (median and Lowess) using default settings with only the mass-to-charge ratio dimension selected. Recalibrated data were interrogated with the Mascot search engine version 2.3.02 (Matrix Science) with a peptide tolerance of ±100 ppm and MS/MS tolerance of ±0.2 D; variable modification was Oxidation (M); up to one missed cleavage for trypsin; and the instrument type was set to electrospray ionization-Q-TOF. Searches were performed against the in-house database as detailed above. A false discovery rate and ion score or expected cutoff were calculated for each experiment using the Decoy feature of Mascot on the MS/MS Ions Search interface. A significance threshold corresponding to a false discovery rate of 5% or less ($P < 0.05$) was used to determine the "Ions Score or Expect Cut-Off" for peptide matches: a value of 30 was used for all three data sets. Ions Score is $-10\log(P)$, where P is the probability that the observed match is a random event. Ions Scores of 30 or greater indicate identity or extensive homology ($P < 0.05$). Specific false discovery rates for peptide matches above the identity threshold were 3.42% for AtGolgi-1, 3.08% for AtGolgi-2, and 3.51% for AtGolgi-3. Data associated with samples in this study (AtGolgi-1, AtGolgi-2, and AtGolgi-3) have been deposited in the PRoteomics IDEntifications (PRIDE) database (Vizcaíno et al., 2010; http://www.ebi.ac.uk/pride/). The three PRIDE data files are derived from concatenated Mascot generic file (mgf) formats exported from Analyst QS 2.0 (AB Sciex) for each fraction analyzed by LC-MS/MS. PRIDE accession numbers are 17168 (AtGolgi-1), 17169 (AtGolgi-2), and 17170 (AtGolgi-3).

Relative Quantitative Analysis of Protein Abundance

Protein abundance in samples analyzed by LC-MS/MS was determined using Scaffold version 3.3.1 (Proteome Software). All data were initially analyzed using the Mascot search engine version 2.3.02 (Matrix Science) against the Arabidopsis protein set (TAIR10) using identical parameters as outlined above. All spectral matches employed $P < 0.05$ to determine the Ions Score or Expect Cut-Off for all peptide matches, resulting in a stringent protein set for each sample. Matched data were imported into the Scaffold software package employing Mascot matching parameters (Ions Score or Expect Cut-Off based on $P < 0.05$ for peptide matches) to define significant protein matches. Data were normalized across each set of biological samples, and quantitation was expressed as "Percentage of Total Spectra" using a "Min # Peptides" of 1 as a filter. A quantitation value for each matched protein was obtained using the average across the biological replicates ($n = 3$) for Supplemental Figure S2. For confidence ranking (Supplemental Fig. S3), each protein from each fraction was assigned a Scaffold quantitation value to generate its distribution profile across FFE fractions.

Assigning Confidence Estimates to Golgi Proteins Separated by FFE

In order to obtain consistent and adequate resolution to determine a protein confidence score and to further demonstrate the reproducibility of the technique, two further independent preparations were enriched for Golgi membranes and analyzed by FFE as previously outlined. From each replicate, 22 fractions encompassing the region representing purified Golgi were analyzed individually by LC-MS/MS. Using relative protein quantitation values, a "Golgi profile" and a "contaminant profile" were generated for both well-known Golgi markers and contaminants across the replicate FFE fractions (Supplemental Fig. S3), against which the profiles for all proteins identified in this Golgi proteome were compared. Each protein was treated as an n-dimensional vector, with the dimensions corresponding to FFE fractions. The protein abundance (normalized spectral counts across each biological sample) of each of the marker proteins was normalized so no one protein would overly skew the distributions (Eq. 1). The percentage Golgi contribution for each fraction was calculated by dividing the Golgi marker protein component by the component from the full list (Eqs. 2 and 3). The similarity between an unknown gene and the Golgi profile is a value between 0 and 1 determined by cosine similarity (Eq. 4). The distribution of raw scores for each protein was broken into fifths to assign final scores on a scale of 1 to 5 at the thresholds of 0.3, 0.45, 0.56, and 0.68.

For calculating organelle profiles from known markers, M_i (vector) = the FFE profile for the ith gene marker for localization, f_j (number) = the protein abundance of a gene marker in the jth FFE fraction, and L (vector) = the localization FFE profile for an organelle:

$$M_i = \frac{\langle f_1, f_2, \ldots, f_j \rangle}{\| \langle f_1, f_2, \ldots, f_j \rangle \|} \quad (1)$$

$$L = \frac{(M_1 + M_2 + \cdots + M_i)}{i} \quad (2)$$

For calculating the Golgi representation of FFE fractions, $L_{G/N}$ (vector) = the FFE profile for Golgi (G) and non-Golgi (N) from Equation 2, $L_G[j]$ (number) = the jth FFE fraction in the localization vector (above), and G (vector) = the Golgi representation of FFE fractions:

$$G = \left\langle \frac{L_G[1]}{(L_G[1] + L_N[1])}, \frac{L_G[2]}{(L_G[2] + L_N[2])}, \frac{L_G[j]}{(L_G[j] + L_N[j])} \right\rangle \quad (3)$$

If $(L_G[j] + L_N[j]) = 0$, the component is set to 0 to avoid division by 0.

For calculating the confidence score, U_i (vector) = the FFE profile for the ith nonmarker gene, calculated by Equation 1, and S_i (number) = the score defining the similarity of the ith unknown to the Golgi localization:

$$S_i = \frac{U_i \cdot G}{\|U_i\| \|G\|} \quad (4)$$

Sequence data from this article can be found in the GenBank/EMBL data libraries under accession numbers JQ937228, JQ937229, JQ937230, JQ937231, JQ937232, JQ937233, JQ937234, JQ937235, JQ937236, JQ937237, JQ937238, JQ937239, JQ937240, and JQ937241.

Supplemental Data

The following materials are available in the online version of this article.

Supplemental Figure S1. Protein localization profiles from pre- and post-FFE Golgi samples.

Supplemental Figure S2. Venn diagram comparison of proteins identified in three Golgi preparations.

Supplemental Figure S3. Estimating confidence for the Golgi proteome by FFE migration.

Supplemental Table S1. All peptide matches from FFE-purified Golgi membranes.

Supplemental Table S2. Golgi proteome and functional breakdown.

Supplemental Table S3. Proteins identified in only a single Golgi preparation by FFE.

Supplemental Table S4. GTs identified in the Golgi proteome.

Supplemental Table S5. PCR primer sets.

ACKNOWLEDGMENTS

We are grateful to the Edinburgh Cell Wall Group (Stephen Fry and Sandra Sharples) for providing the Arabidopsis cell cultures. We also appreciate the kind gift of the α-ManI antibody from the Bednarek Laboratory (Sebastian Bednarek and Colleen McMichael) from the University of Wisconsin, Madison.

Received January 4, 2012; accepted March 4, 2012; published March 19, 2012.

LITERATURE CITED

Abeijon C, Yanagisawa K, Mandon EC, Häusler A, Moremen K, Hirschberg CB, Robbins PW (1993) Guanosine diphosphatase is required for protein and sphingolipid glycosylation in the Golgi lumen of *Saccharomyces cerevisiae*. J Cell Biol **122:** 307–323

Abramoff MD, Magalhaes PJ, Ram SJ (2004) Image processing with ImageJ. Biophotonics Int **11:** 36–42

Asakura T, Hirose S, Katamine H, Kitajima A, Hori H, Sato MH, Fujiwara M, Shimamoto K, Mitsui T (2006) Isolation and proteomic analysis of rice Golgi membranes: cis-Golgi membranes labeled with GFP-SYP31. Plant Biotechnol **23:** 475–485

Avisar D, Prokhnevsky AI, Makarova KS, Koonin EV, Dolja VV (2008) Myosin XI-K is required for rapid trafficking of Golgi stacks, peroxisomes, and mitochondria in leaf cells of *Nicotiana benthamiana*. Plant Physiol **146:** 1098–1108

Baginsky S, Gruissem W (2006) *Arabidopsis thaliana* proteomics: from proteome to genome. J Exp Bot **57:** 1485–1491

Bardy N, Carrasco A, Galaud JP, Pont-Lezica R, Canut H (1998) Free-flow electrophoresis for fractionation of *Arabidopsis thaliana* membranes. Electrophoresis **19:** 1145–1153

Barkla BJ, Vera-Estrella R, Pantoja O (2007) Enhanced separation of membranes during free flow zonal electrophoresis in plants. Anal Chem **79:** 5181–5187

Blanch HW, Adams PD, Andrews-Cramer KM, Frommer WB, Simmons BA, Keasling JD (2008) Addressing the need for alternative transportation fuels: the Joint BioEnergy Institute. ACS Chem Biol **3:** 17–20

Boevink P, Oparka K, Santa Cruz S, Martin B, Betteridge A, Hawes C (1998) Stacks on tracks: the plant Golgi apparatus traffics on an actin/ER network. Plant J **15:** 441–447

Caffall KH, Pattathil S, Phillips SE, Hahn MG, Mohnen D (2009) *Arabidopsis thaliana* T-DNA mutants implicate GAUT genes in the biosynthesis of pectin and xylan in cell walls and seed testa. Mol Plant **2:** 1000–1014

Cantarel BL, Coutinho PM, Rancurel C, Bernard T, Lombard V, Henrissat B (2009) The Carbohydrate-Active EnZymes database (CAZy): an expert resource for glycogenomics. Nucleic Acids Res **37:** D233–D238

Canut H, Bauer J, Weber G (1999) Separation of plant membranes by electromigration techniques. J Chromatogr B Biomed Sci Appl **722:** 121–139

Canut H, Brightman A, Boudet AM, Morré DJ (1988) Plasma membrane vesicles of opposite sidedness from soybean hypocotyls by preparative free-flow electrophoresis. Plant Physiol **86:** 631–637

Canut H, Brightman A, Boudet AM, Morré DJ (1990) Tonoplast vesicles of opposite sidedness from soybean hypocotyls by preparative free-flow electrophoresis. Plant Physiol **94:** 1149–1156

Carter C, Pan SQ, Zouhar J, Avila EL, Girke T, Raikhel NV (2004) The vegetative vacuole proteome of *Arabidopsis thaliana* reveals predicted and unexpected proteins. Plant Cell **16:** 3285–3303

Chen XY, Liu L, Lee E, Han X, Rim Y, Chu H, Kim SW, Sack F, Kim JY (2009) The Arabidopsis callose synthase gene *GSL8* is required for cytokinesis and cell patterning. Plant Physiol **150:** 105–113

Cocuron JC, Lerouxel O, Drakakaki G, Alonso AP, Liepman AH, Keegstra K, Raikhel N, Wilkerson CG (2007) A gene from the cellulose synthase-like C family encodes a beta-1,4 glucan synthase. Proc Natl Acad Sci USA **104:** 8550–8555

Desprez T, Juraniec M, Crowell EF, Jouy H, Pochylova Z, Parcy F, Höfte H, Gonneau M, Vernhettes S (2007) Organization of cellulose synthase complexes involved in primary cell wall synthesis in *Arabidopsis thaliana*. Proc Natl Acad Sci USA **104:** 15572–15577

Dunkley TP, Watson R, Griffin JL, Dupree P, Lilley KS (2004) Localization of organelle proteins by isotope tagging (LOPIT). Mol Cell Proteomics **3:** 1128–1134

Dunkley TPJ, Hester S, Shadforth IP, Runions J, Weimar T, Hanton SL, Griffin JL, Bessant C, Brandizzi F, Hawes C, et al (2006) Mapping the Arabidopsis organelle proteome. Proc Natl Acad Sci USA **103:** 6518–6523

Eubel H, Lee CP, Kuo J, Meyer EH, Taylor NL, Millar AH (2007) Free-flow electrophoresis for purification of plant mitochondria by surface charge. Plant J **52:** 583–594

Eubel H, Meyer EH, Taylor NL, Bussell JD, O'Toole N, Heazlewood JL, Castleden I, Small ID, Smith SM, Millar AH (2008) Novel proteins, putative membrane transporters, and an integrated metabolic network are revealed by quantitative proteomic analysis of Arabidopsis cell culture peroxisomes. Plant Physiol **148:** 1809–1829

Eudes A, Baidoo EE, Yang F, Burd H, Hadi MZ, Collins FW, Keasling JD, Loqué D (2011) Production of tranilast [N-(3′,4′-dimethoxycinnamoyl)-anthranilic acid] and its analogs in yeast *Saccharomyces cerevisiae*. Appl Microbiol Biotechnol **89:** 989–1000

Frand AR, Cuozzo JW, Kaiser CA (2000) Pathways for protein disulphide bond formation. Trends Cell Biol **10:** 203–210

Galat A, Metcalfe SM (1995) Peptidylproline cis/trans isomerases. Prog Biophys Mol Biol **63:** 67–118

Gibeaut DM, Carpita NC (1990) Separation of membranes by flotation centrifugation for *in vitro* synthesis of plant-cell wall polysaccharides. Protoplasma **156:** 82–93

Gietz RD, Sugino A (1988) New yeast-*Escherichia coli* shuttle vectors constructed with in vitro mutagenized yeast genes lacking six-base pair restriction sites. Gene **74:** 527–534

Gietz RD, Woods RA (2002) Transformation of yeast by lithium acetate/single-stranded carrier DNA/polyethylene glycol method. *In* G Christine, RF Gerald, eds, Methods in Enzymology, Vol 350. Elsevier, Amsterdam, pp 87–96

Hansen SF, Bettler E, Wimmerová M, Imberty A, Lerouxel O, Breton C (2009) Combination of several bioinformatics approaches for the identification of new putative glycosyltransferases in Arabidopsis. J Proteome Res **8:** 743–753

Harholt J, Jensen JK, Sørensen SO, Orfila C, Pauly M, Scheller HV (2006) ARABINAN DEFICIENT 1 is a putative arabinosyltransferase involved in biosynthesis of pectic arabinan in Arabidopsis. Plant Physiol **140:** 49–58

Hawes C, Brandizzi F (2004) The Golgi apparatus: still causing problems after all these years! Cell Mol Life Sci **61:** 131–132

Heazlewood JL, Tonti-Filippini JS, Gout AM, Day DA, Whelan J, Millar AH (2004) Experimental analysis of the *Arabidopsis* mitochondrial proteome highlights signaling and regulatory components, provides assessment of targeting prediction programs, and indicates plant-specific mitochondrial proteins. Plant Cell **16:** 241–256

Heazlewood JL, Verboom RE, Tonti-Filippini J, Small I, Millar AH (2007) SUBA: the Arabidopsis subcellular database. Nucleic Acids Res **35:** D213–D218

Herrero AB, Uccelletti D, Hirschberg CB, Dominguez A, Abeijon C (2002) The Golgi GDPase of the fungal pathogen *Candida albicans* affects morphogenesis, glycosylation, and cell wall properties. Eukaryot Cell **1:** 420–431

Huang S, Taylor NL, Narsai R, Eubel H, Whelan J, Millar AH (2009) Experimental analysis of the rice mitochondrial proteome, its biogenesis, and heterogeneity. Plant Physiol **149:** 719–734

Islinger M, Eckerskorn C, Völkl A (2010) Free-flow electrophoresis in the proteomic era: a technique in flux. Electrophoresis **31:** 1754–1763

Ito J, Batth TS, Petzold CJ, Redding-Johanson AM, Mukhopadhyay A, Verboom R, Meyer EH, Millar AH, Heazlewood JL (2011) Analysis of the Arabidopsis cytosolic proteome highlights subcellular partitioning of central plant metabolism. J Proteome Res **10:** 1571–1582

Jaquinod M, Villiers F, Kieffer-Jaquinod S, Hugouvieux V, Bruley C, Garin J, Bourguignon J (2007) A proteomics dissection of *Arabidopsis thaliana* vacuoles isolated from cell culture. Mol Cell Proteomics **6:** 394–412

Jelitto-Van Dooren EPWM, Vidal S, Denecke J (1999) Anticipating endoplasmic reticulum stress: a novel early response before pathogenesis-related gene induction. Plant Cell **11:** 1935–1944

Kang JS, Frank J, Kang CH, Kajiura H, Vikram M, Ueda A, Kim S, Bahk JD, Triplett B, Fujiyama K, et al (2008) Salt tolerance of Arabidopsis thaliana requires maturation of N-glycosylated proteins in the Golgi apparatus. Proc Natl Acad Sci USA **105:** 5933–5938

Lalonde S, Sero A, Pratelli R, Pilot G, Chen J, Sardi MI, Parsa SA, Kim D-Y, Acharya BR, Stein EV, et al (2010) A membrane protein/signaling protein interaction network for Arabidopsis version AMPv2. Front Physiol **1:** 24

Liepman AH, Wilkerson CG, Keegstra K (2005) Expression of cellulose synthase-like (Csl) genes in insect cells reveals that CslA family members encode mannan synthases. Proc Natl Acad Sci USA **102:** 2221–2226

Loqué D, Lalonde S, Looger LL, von Wirén N, Frommer WB (2007) A cytosolic trans-activation domain essential for ammonium uptake. Nature **446:** 195–198

Marmagne A, Ferro M, Meinnel T, Bruley C, Kuhn L, Garin J, Barbier-Brygoo H, Ephritikhine G (2007) A high content in lipid-modified peripheral proteins and integral receptor kinases features in the Arabidopsis plasma membrane proteome. Mol Cell Proteomics **6:** 1980–1996

Matheson LA, Hanton SL, Brandizzi F (2006) Traffic between the plant endoplasmic reticulum and Golgi apparatus: to the Golgi and beyond. Curr Opin Plant Biol **9:** 601–609

Meyer EH, Millar AH (2008) Isolation of mitochondria from plant cell culture. Methods Mol Biol **425:** 163–169

Mitra SK, Walters BT, Clouse SD, Goshe MB (2009) An efficient organic solvent based extraction method for the proteomic analysis of Arabidopsis plasma membranes. J Proteome Res **8:** 2752–2767

Mohnen D (2008) Pectin structure and biosynthesis. Curr Opin Plant Biol **11:** 266–277

Morre DJ, Mollenhauer HH (1964) Isolation of Golgi apparatus from plant cells. J Cell Biol **23:** 295–305

Morre DJ, Mollenhauer HH (2009) The Golgi Apparatus: The First 100 Years. Springer, New York

Mortimer JC, Miles GP, Brown DM, Zhang ZN, Segura MP, Weimar T, Yu XL, Seffen KA, Stephens E, Turner SR, et al (2010) Absence of branches from xylan in Arabidopsis gux mutants reveals potential for simplification of lignocellulosic biomass. Proc Natl Acad Sci USA **107:** 17409–17414

Munoz P, Norambuena L, Orellana A (1996) Evidence for a UDP-glucose transporter in Golgi apparatus-derived vesicles from pea and its possible role in polysaccharide biosynthesis. Plant Physiol **112:** 1585–1594

Nanjo Y, Oka H, Ikarashi N, Kaneko K, Kitajima A, Mitsui T, Muñoz FJ, Rodríguez-López M, Baroja-Fernández E, Pozueta-Romero J (2006) Rice plastidial N-glycosylated nucleotide pyrophosphatase/phosphodiesterase is transported from the ER-Golgi to the chloroplast through the secretory pathway. Plant Cell **18:** 2582–2592

Nelson BK, Cai X, Nebenführ A (2007) A multicolored set of in vivo organelle markers for co-localization studies in Arabidopsis and other plants. Plant J **51:** 1126–1136

Oikawa A, Joshi HJ, Rennie EA, Ebert B, Manisseri C, Heazlewood JL, Scheller HV (2010) An integrative approach to the identification of Arabidopsis and rice genes involved in xylan and secondary wall development. PLoS ONE **5:** e15481

Ondzighi CA, Christopher DA, Cho EJ, Chang SC, Staehelin LA (2008) *Arabidopsis* protein disulfide isomerase-5 inhibits cysteine proteases during trafficking to vacuoles before programmed cell death of the endothelium in developing seeds. Plant Cell **20:** 2205–2220

Paredez AR, Somerville CR, Ehrhardt DW (2006) Visualization of cellulose synthase demonstrates functional association with microtubules. Science **312:** 1491–1495

Persson S, Paredez A, Carroll A, Palsdottir H, Doblin M, Poindexter P, Khitrov N, Auer M, Somerville CR (2007) Genetic evidence for three unique components in primary cell-wall cellulose synthase complexes in Arabidopsis. Proc Natl Acad Sci USA **104:** 15566–15571

Petyuk VA, Mayampurath AM, Monroe ME, Polpitiya AD, Purvine SO, Anderson GA, Camp DG II, Smith RD (2010) DtaRefinery, a software tool for elimination of systematic errors from parent ion mass measurements in tandem mass spectra data sets. Mol Cell Proteomics **9:** 486–496

Pimpl P, Taylor JP, Snowden C, Hillmer S, Robinson DG, Denecke J (2006) Golgi-mediated vacuolar sorting of the endoplasmic reticulum chaperone BiP may play an active role in quality control within the secretory pathway. Plant Cell **18:** 198–211

Rentsch D, Laloi M, Rouhara I, Schmelzer E, Delrot S, Frommer WB (1995) NTR1 encodes a high affinity oligopeptide transporter in Arabidopsis. FEBS Lett **370:** 264–268

Reyes F, Orellana A (2008) Golgi transporters: opening the gate to cell wall polysaccharide biosynthesis. Curr Opin Plant Biol **11:** 244–251

Robinson DG, Herranz MC, Bubeck J, Pepperkok R, Ritzenthaler C (2007) Membrane dynamics in the early secretory pathway. Crit Rev Plant Sci **26:** 199–225

Saint-Jore-Dupas C, Nebenführ A, Boulaflous A, Follet-Gueye ML, Plasson C, Hawes C, Driouich A, Faye L, Gomord V (2006) Plant N-glycan processing enzymes employ different targeting mechanisms for their spatial arrangement along the secretory pathway. Plant Cell **18:** 3182–3200

Schaller GE, DeWitt ND (1995) Analysis of the H^+-ATPase and other proteins of the Arabidopsis plasma membrane. *In* DW Galbraith, DP Bourque, HJ Bohnert, eds, Methods in Plant Cell Biology, Vol 50. Academic Press, San Diego, pp 129–148

Scheible WR, Pauly M (2004) Glycosyltransferases and cell wall biosynthesis: novel players and insights. Curr Opin Plant Biol **7:** 285–295

Scheller HV, Jensen JK, Sorensen SO, Harholt J, Geshi N (2007) Biosynthesis of pectin. Physiol Plant **129:** 283–295

Seifert GJ, Roberts K (2007) The biology of arabinogalactan proteins. Annu Rev Plant Biol **58:** 137–161

Steinebrunner I, Jeter C, Song C, Roux SJ (2000) Molecular and biochemical comparison of two different apyrases from Arabidopsis thaliana. Plant Physiol Biochem **38:** 913–922

Sterling JD, Atmodjo MA, Inwood SE, Kumar Kolli VS, Quigley HF, Hahn MG, Mohnen D (2006) Functional identification of an Arabidopsis pectin biosynthetic homogalacturonan galacturonosyltransferase. Proc Natl Acad Sci USA **103:** 5236–5241

Strasser R (2009) Localization of plant N-glycan processing enzymes along the secretory pathway. Plant Biosyst **143:** 636–642

Strompen G, Dettmer J, Stierhof YD, Schumacher K, Jürgens G, Mayer U (2005) Arabidopsis vacuolar H-ATPase subunit E isoform 1 is required for Golgi organization and vacuole function in embryogenesis. Plant J **41:** 125–132

Sze H, Schumacher K, Müller ML, Padmanaban S, Taiz L (2002) A simple nomenclature for a complex proton pump: VHA genes encode the vacuolar $H(^+)$-ATPase. Trends Plant Sci **7:** 157–161

Thimm O, Bläsing O, Gibon Y, Nagel A, Meyer S, Krüger P, Selbig J, Müller LA, Rhee SY, Stitt M (2004) MAPMAN: a user-driven tool to display genomics data sets onto diagrams of metabolic pathways and other biological processes. Plant J **37:** 914–939

Turano C, Coppari S, Altieri F, Ferraro A (2002) Proteins of the PDI family: unpredicted non-ER locations and functions. J Cell Physiol **193:** 154–163

Vizcaíno JA, Côté R, Reisinger F, Barsnes H, Foster JM, Rameseder J, Hermjakob H, Martens L (2010) The Proteomics Identifications database: 2010 update. Nucleic Acids Res **38:** D736–D742

Wang HZ, Boavida LC, Ron M, McCormick S (2008) Truncation of a protein disulfide isomerase, PDIL2-1, delays embryo sac maturation and disrupts pollen tube guidance in *Arabidopsis thaliana*. Plant Cell **20:** 3300–3311

Wang Y, Shao L, Shi SL, Harris RJ, Spellman MW, Stanley P, Haltiwanger RS (2001) Modification of epidermal growth factor-like repeats with O-fucose: molecular cloning and expression of a novel GDP-fucose protein O-fucosyltransferase. J Biol Chem **276:** 40338–40345

Willats WGT, Steele-King CG, Marcus SE, Knox JP (1999) Side chains of pectic polysaccharides are regulated in relation to cell proliferation and cell differentiation. Plant J **20:** 619–628

Wolf C, Hennig M, Romanovicz D, Steinebrunner I (2007) Developmental defects and seedling lethality in apyrase AtAPY1 and AtAPY2 double knockout mutants. Plant Mol Biol **64:** 657–672

Wu AM, Hörnblad E, Voxeur A, Gerber L, Rihouey C, Lerouge P, Marchant A (2010a) Analysis of the Arabidopsis IRX9/IRX9-L and

IRX14/IRX14-L pairs of glycosyltransferase genes reveals critical contributions to biosynthesis of the hemicellulose glucuronoxylan. Plant Physiol **153:** 542–554

Wu CC, MacCoss MJ, Mardones G, Finnigan C, Mogelsvang S, Yates JR III, Howell KE (2004) Organellar proteomics reveals Golgi arginine dimethylation. Mol Biol Cell **15:** 2907–2919

Wu J, Steinebrunner I, Sun Y, Butterfield T, Torres J, Arnold D, Gonzalez A, Jacob F, Reichler S, Roux SJ (2007) Apyrases (nucleoside triphosphate-diphosphohydrolases) play a key role in growth control in Arabidopsis. Plant Physiol **144:** 961–975

Wu Y, Williams M, Bernard S, Driouich A, Showalter AM, Faik A (2010b) Functional identification of two nonredundant Arabidopsis alpha(1,2) fucosyltransferases specific to arabinogalactan proteins. J Biol Chem **285:** 13638–13645

Yeh JC, Ong E, Fukuda M (1999) Molecular cloning and expression of a novel beta-1,6-N-acetylglucosaminyltransferase that forms core 2, core 4, and I branches. J Biol Chem **274:** 3215–3221

Yin YB, Chen HL, Hahn MG, Mohnen D, Xu Y (2010) Evolution and function of the plant cell wall synthesis-related glycosyltransferase family 8. Plant Physiol **153:** 1729–1746

Zhou YH, Li SB, Qian Q, Zeng DL, Zhang M, Guo LB, Liu XL, Zhang BC, Deng LW, Liu XF, et al (2009) BC10, a DUF266-containing and Golgi-located type II membrane protein, is required for cell-wall biosynthesis in rice (*Oryza sativa* L.). Plant J **57:** 446–462